SSRG International Journal of Electrical and Electronics Engineering
ISSN: 2348-8379/ https://doi.org/10.14445/23488379/IJEEE-V10I10P121

Volume 10 Issue 10, 227-240, October 2023
© 2023 Seventh Sense Research Group®

Original Article

Opposition Based Modified Rao's Algorithm for Optimal Power Flow Incorporating C-UPFC

Shaik Mabhu Jani[1], K. Rama Sudha[2], K. Padma[3], A. Chandra Sekhar[4]

[1,2,3]*Department of Electrical Engineering, Andhra University College of Engineering, Visakhapatnam, India.*
[4]*Department of Mathematics, GITAM University, Visakhapatnam, India.*

[2]*Corresponding Author : prof.kramasudha@andhrauniversity.edu.in*

Received: 20 August 2023 Revised: 24 September 2023 Accepted: 17 October 2023 Published: 31 October 2023

Abstract *- In power system monitoring, operation, design and expansion, Optimal Power Flow (OPF) is vital. The present paper proposes an Opposition-based Modified Rao's algorithm (OMR) for OPF solution incorporating a Centre node Unified Power Flow Controller (C-UPFC) device. In this paper, objectives such as total generation cost, total actual power loss, the sum of squared voltage stability index, and total voltage deviation are optimized, and performance parameters in terms of real and reactive power flows, voltage profile, load bus voltage deviations, load angle and voltage stability indices using the proposed OMR algorithm. The efficacy of the proposed technique is tested on the IEEE-30 standard bus system and compared with other techniques reported in this paper. The results obtained with the proposed OMR algorithm yield better results than the other techniques.*

Keywords *- C-UPFC device, FACTS, Opposition based Modified Rao's algorithm (OMR), Optimal Power Flow (OPF), Power system.*

1. Introduction

A significant aspect for decision-makers and operators in power systems is Optimal Power Flow (OPF). Solution to the OPF problem implies assigning an optimal operating point to reduce voltage deviations, power losses, fuel cost, emission, and system stability enhancement. Transformer tap-ratio, the output power of generation units, compensation units' Var outputs, and generating system voltages are parameters that can address the required objective function. OPF problem is challenging; many efforts have been invested to solve it, like developing various numerical and optimization techniques. Some are linear & nonlinear programming, interior point methodology, quadratic programming, and Newton-based techniques [1].

However, these methods pose unwanted issues like unsettling convergence, unsuitable for nonlinear functions, and stagnation at local optima. Hence, the OPF problem is solved using meta-heuristic techniques. They may be categorized as evolutionary, physical, and human-based algorithms per the method's inherent inspiration. Evolutionary programming and Genetic Algorithm (GA) are a few evolutionary algorithms developed as alternates to conventional algorithms. However, these algorithms provide 'near global' optimum values but not actual global optimum values. PSO is a worldwide search optimization algorithm that is fast and simple compared to other techniques, giving promising results. Reference [2], Matlab software describes and contrasts A conventional matrix-implemented Static synchronous Compensator (STATCOM) model and a STATCOM model with a small signal.

Reference [3], the OPF problem is solved using PSO based method for the system with STATCOM to minimize the power losses and maintain the system's stability. Ref [4], The effect of STATCOM is examined on the SCIG wind-farm connected system using a STATCOM model.

In [5], Chemical reaction optimization is used to minimize the active power loss by proper sizing and location of the Static Synchronous Series Compensator (SSSC) for optimal reactive power dispatch in IEEE 30-bus and 57-bus systems. The PI controller is used for current mode control of reactive and absolute power of the system with SSSC to improve the power transmission capacity [6]. Power quality is enhanced by eliminating flickers caused by electric arc furnaces by Static VAR Compensator (SVC) [7].

Transient stability improved in the power system in [8] by SVC. Unified Power Flow Controller (UPFC) location is determined to improve the power quality using different metaheuristic algorithms [9]. In [10], the UPFC model based on the current injection method is presented to

This is an open access article under the CC BY-NC-ND license (http://creativecommons.org/licenses/by-nc-nd/4.0/)

analyze the power solution using the criss cross optimization technique. In [11], Optimal UPFC was used for the multi-objective firefly algorithm in IEEE 14-bus and New England 39-bus systems for actual power loss and voltage stability limit optimization.

Evolutionary programming in [12] is used for optimal sitting of UPFC in the IEEE 14-bus reliability test system to improve voltage stability and power minimization. OPF problem is solved by Modified Jaya algorithm (MJAYA) in IEEE-30 and IEEE-118 bus systems with and without adding of renewable energy sources for OPF problem and improvement of voltage profile and minimization of fuel cost and losses are chosen as objective functions in [13].

In [14], multi-objective OPF is solved by using an enhanced self-adaptive differential evolution algorithm and Modified Rao-2 (MRao-2) algorithm employed in [15] for OPF problem in the IEEE-30 and IEEE-118 bus systems with and without consideration of renewable energy sources. The suggested method was improved using Quasi-oppositional and Levy flight methods and compared with the recent techniques mentioned in [15] that paper. In [16], an opposition-based differential evolution algorithm is proposed to improve the differential evolution algorithm.

Despite the UPFC being regarded as a better and adaptable FACTS device, new iterations, such as the Generalized Unified Power Flow Controller (GUPFC) and C-UPFC, are introduced to use the UPFC's device potential fully. GUPFC is a Multi-Voltage Source Converter (VSC) FACTS device employed to manage various characteristics of lines and buses based on the quantity of both shunt and series VSCs. PSO algorithm is applied for the optimal location of GUPFC, and its parameters for transmission loss minimization in the IEEE-14 bus system in [17, 18], power injection-based GUPFC model is used to maximize power system efficiency and reliability in the IEEE 30-bus system.

C-UPFC is another modified version of the UPFC device. At the Centre of the transmission line, a C-UPFC, a powerful controller, is connected in series to regulate the power flow and voltage [19-20]. A few publications have presented the modelling and assessment of the C-UPFC controller to improve power transfer capability. Reference [21], In a transmission line to regulate power flow, an effectual C-UPFC model was introduced. References [22, 23], a representation of C-UPFC in the Newton-Raphson power flow method has been addressed, depending on the injected power model.

Metaheuristic algorithms use self-algorithm parameters, so the computational time increases and takes more time for convergence. To overcome this, the proposed work uses a less self-algorithm parameters-based optimization technique, i.e., Rao's algorithm. Rao's algorithm is simple, using only common data like the size of the population, variable length and termination criteria. It takes less time compared to metaheuristic optimization techniques and has faster convergence characteristics than metaheuristic techniques. To enhance Rao's algorithm performance, Modified Rao's algorithm is being used for speed convergence. For a further enhancement to Rao's algorithm, in this paper, a novel approach with Opposition-based Modified Rao's algorithm is proposed to solve the OPF problem.

This paper considers the IEEE-30 bus standard test system to determine the effectiveness of the proposed Opposition-based Modified Rao algorithms. Here, the different objectives like total fuel cost generation, total actual power loss, the sum of squared voltage stability index and absolute voltage deviation are formulated to optimize individually with various constraints and performance parameters are also obtained. The best outcomes from the proposed Opposition-based Modified Rao's algorithm compared with those reported in the literature review. With this, it observed that the proposed OMR algorithm performs better regarding objectives, system performance and execution times.

1.1. Summary of This Paper is as Follows

- A C-UPFC model is used to address the OPF problem, and one of the model's key advantages is that it avoids the need for complicated alternations to load flow in section 2.
- A unique version of Rao's algorithm that is an Opposition-based Modified Rao's algorithm proposed for improving the performance of Rao's algorithm.
- The suggested approach is evaluated on the standard IEEE-30 bus system and successfully applied to the OPF problem, and the OPF solution by the OMR algorithm is discussed in detail.
- The OMR algorithm's results regarding fuel cost, power loss, sum of squared voltage stability index, and total voltage deviation are obtained.

1.2. The Organization of This Paper is as Follows

- Introduction to the paper is provided in Section 1.
- Introduction to C-UPFC is provided in Section 2.
- Mathematical model of the C-UPFC device is in section 3.
- Mathematical formulations for the problem of optimal power flow are provided in section 4.
- The proposed OMR algorithm is introduced in Section 5.
- The obtained results are discussed and compared with other techniques mentioned in the literature in section 6.
- The overall conclusion of the paper is provided in section 7.

2. Center Node Unified Power Flow Controller

The most recent FACTS device for regulating actual power flow and voltage magnitude in lines and buses is C-UPFC. UPFC's fundamental derivative device is C-UPFC.

However, in C-UPFC, the connection of this device is inset in succession with the transmission line and connected autonomously in the middle of the transmission line to regulate voltage and power flow. Therefore, C-UPFC can maintain the AC voltage at the line's midpoint, the reactive power flow at the line's ends and the active power.

Reference [19] implements a FACTS structure at the transmission line's middle point. Adjusting voltage increases the transmission limit at the mid-line depending on the transmission angle. Based on this, a new method called C-UPFC to increase the voltage compensation spectrum without violating the voltage margin was proposed by B. T. Ooi B. Lu [20].

In [24], the Adaptive Grasshopper Optimization (AGOA) algorithm is used for OPF problems with C-UPFC in IEEE 30-bus, 57-bus and 26-bus systems. For conventional GOA, levy flight distribution and search agents spiral path orientation applied to overcome the stagnation problem and increase its ability to search and fuel cost, emission, piece-wise cost, and fuel cost with valve point considered objective functions.

Levy spiral flight equilibrium optimizer is used in [25] for the OPF problem and determines the optimal location of C-UPFC for the IEEE-30 bus system. Levy flight and spiral motion of particles are used to improve the Equilibrium optimizer performance, and fuel cost, voltage deviation, and power losses are taken as objective functions.

The major disadvantage of a model of the UPFC is that it cannot be modified to function simultaneously in voltage control, impedance compensation, and phase shift modes. It maintains the power flow and voltage in the transmission line when one device is connected in a shunt, and when the other is connected in series, it controls this in one direction only.

At the same time, the C-UPFC device is considered one of the modernist members of the Flexible AC Transmission System (FACTS). In this, two devices are connected in series and one in shunt to control the power flow in the lines and voltage in the bus. One of the significant benefits of a C-UPFC device is that it has the potential to singly control various system elements, i.e., voltage magnitude at the transmission line mid-point, flow of absolute power through the transmission line and reactive power at the transmission line on both ends.

This paper details the proposed OMR optimization algorithm using C-UPFC optimizing the objectives such as total generation fuel cost, active power loss, voltage stability index and total voltage deviation. A standard IEEE-30 bus-tested system is considered to test the proposed algorithm. The results obtained with the OMR algorithm using the C-UPFC device are effectively superior solutions compared to recent algorithms and other meta-heuristic approaches reported in the literature.

3. Mathematical Modelling of C-UPFC Device

The C-UPFC FACTS device model is based on controlling four parameters: the magnitude of the mid-point voltage, flow of absolute power in the transmission line, flow of reactive power at the sending end and flow of reactive power at the receiving end connected in succession at the mid-point of the transmission line [19, 20].

Figure 1 shows a DC storage capacitor provides a common DC link for the C-UPFC, which has three voltage source converters connected to it. Two series converters at the line's ends control the reactive and active power of the system, while a shunt converter at the line's midpoint regulates the voltage magnitude.

A shunt converter's primary job is to absorb or inject active power demand into a common DC link via a series converter to help with active power exchange through series voltage injection.

Figure 2 shows the primary node point of the C-UPFC device, represented by three buses (bus k, l and m) to adjust the power flow via the transmission line. Bus k is PV type of bus, and bus l and m are the PQ bus type. The mathematical series converter model is displayed according to (1) and (2).

$$I_{sen} = \frac{V_{sen}}{jX_{sen}} \tag{1}$$

$$I_{rec} = \frac{V_{rec}}{jX_{rec}} \tag{2}$$

Figure 3 shows that the current source is converted into a shunt, and then the specified values are calculated using Kirchhoff's current law at the bus (k and m).

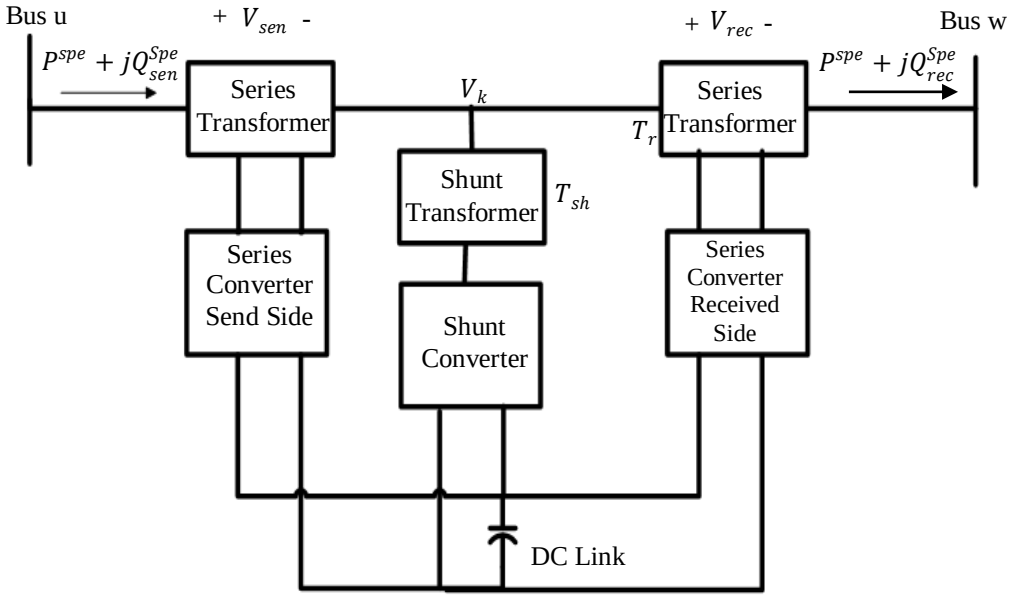

Fig. 1 C-UPFC device structure

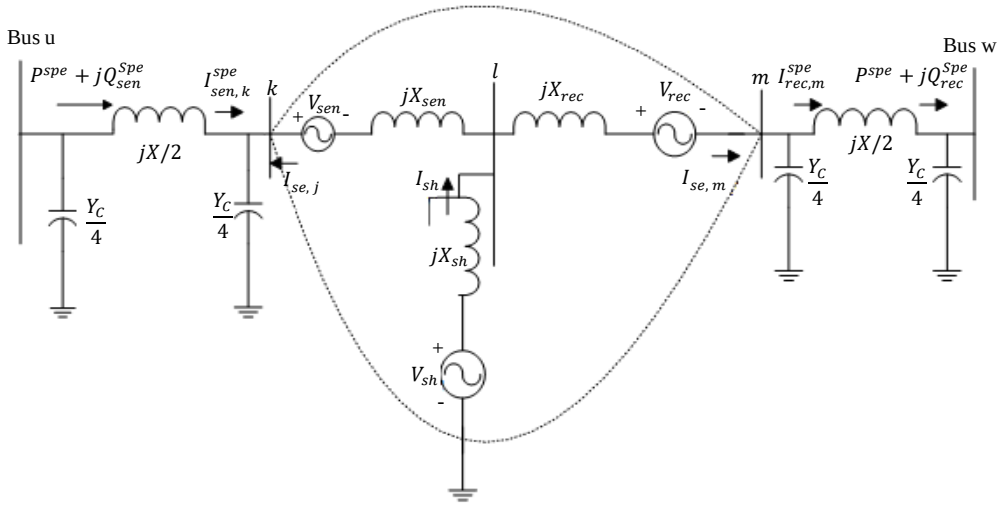

Fig. 2 C-UPFC device voltage source

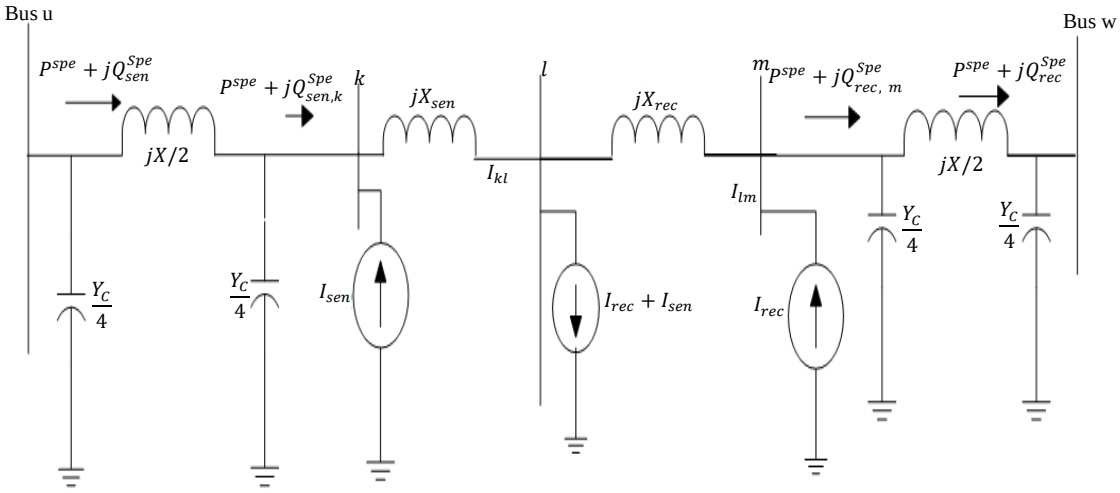

Fig. 3 Shunt injected current representation of series converter

By making use of Kirchhoff's current law at bus k:

$$I_{sen} = I_{kl} — I_{sen,k}^{spe} = \frac{V_k — V_l}{jX_{sen}} \left[\frac{S_{sen,k}^{spe}}{V_k}\right]^* \quad (3)$$

Where,

$$S_{sen,k}^{spe} = — P^{spe} + jQ_{sen,k}^{spe} \quad (4)$$

$$Q_{sen,k}^{spe} = Q_{sen}^{spe} + V_u^2 \frac{B}{4} — I_{uk}^2 \frac{X}{2} + V_k^2 \frac{B}{4} \quad (5)$$

Kirchhoff's Current Law is applied at bus m:

$$I_{se2} = I_{rec} = I_{rec,m}^{spe} — I_{lm} = \left[\frac{S_{rec,m}^{spe}}{V_m}\right]^* — \frac{V_l — V_m}{jX_{rec}} \quad (6)$$

Where

$$I_{rec,m}^{spe} = \left[\frac{S_{rec,m}^{spe}}{V_m}\right]^* \quad (7)$$

$$S_{rec,m}^{spe} = P^{spe} + jQ_{rec,m}^{spe} \quad (8)$$

$$Q_{rec,m}^{spe} = Q_{rec}^{spe} — V_w^2 \frac{B}{4} — I_{wm}^2 \frac{X}{2} V_m^2 \frac{B}{4} \quad (9)$$

The shunt current, considering the complex load, can be

$$\left.\begin{aligned} S_k &= -V_k \times (I_{sen})^* \\ S_m &= -V_m \times (I_{rec})^* \\ S_l &= V_l \times (I_{sen} + I_{rec})^* \end{aligned}\right\} \quad (10)$$

By replacing the I_{rec} and I_{sen} values from (2) and (1), the series injected voltage is determined according to equations (11) and (12) at the sending and receiving ends.

$$V_{sen} = -\left(\frac{S_{sen,k}^{spe}}{V_k}\right)^* \times jX_{sen} + V_k — V_l \quad (11)$$

$$V_{rec} = -\left(\frac{S_{rec,m}^{spe}}{V_m}\right)^* \times jX_{sen} — V_l + V_m \quad (12)$$

$$\left.\begin{aligned} p_{ex1} &= Re(V_{sen}(I_{se1})^*) \\ p_{ex2} &= Re(V_{rec}(I_{se2})^*) \end{aligned}\right\} \quad (13)$$

The net real power exchange between the system and the controller is zero, ignoring the converter loss. The shunt power to connect the system can be,

$$P_l^{load} = P_l — P_{sh}, Q_l^{load} = Q_l \quad (14)$$

The key function of the shunt power is to balance the power flow through the converter. The injected load at the midpoint of the connection.

$$P_l^{load} = P_l — P_{sh}, Q_l^{load} = Q_l \quad (15)$$

From Figure 4, the reactive power created using the reactive balance power at the mid-point, which is described by,

$$\begin{aligned} Q_{sh} = {} & V_l V_k (G_{kl} \sin\delta_{kl} — B_{kl} \cos\delta_{kl}) + \\ & V_l V_m (G_{ml} \sin\delta_{ml} — B_{ml} \cos\delta_{ml}) + Q_l^{load} \end{aligned} \quad (16)$$

Finally, by discussing Figure 1, the injected shunt current and voltage can be described in the following (17) and (18)

$$I_{sh} = I_{se1} + I_{se2} \quad (17)$$

$$V_{sh} = V_l + jX_{sh}\left(\frac{P_{sh} + jQ_{sh}}{V_l}\right) \quad (18)$$

Figure 4 shows the proposed model of the C-UPFC device. Hence, the injected load, i.e. S_k, S_m, P_l^{Load} and produced reactive power (Q_{sh}) at bus j are characteristics of C-UPFC. These are all updated as $P^{spe}, Q_{sen}^{spe}, Q_{rec}^{spe}$ and V_l and accounted for in the power mismatch vector of the Newton-Raphson method.

4. A Mathematical Formulation of Optimal Power Flow Problem

The problem of optimal power flow is mainly concerned with power losses in the system and reducing the active generation fuel cost for the given system operating limits.

The total generation fuel cost can be written as:

$$f_1 = F(P_G) = \left(\sum_{k=1}^{NG} d_k P_{gk}^2 + e_k P_{gk} + h_k\right)\$/h \quad (19)$$

Where d_k, e_k, and h_k are the coefficients for the fuel cost of the k^{th}generator. The calculation of a transmission line's overall active power loss is given below.

$$\begin{aligned} f_2 = P_{loss}(k) = {} & \sum_{\substack{l=1 \\ k\neq l}}^{nl} g_{k.l} (V_k^2 + V_l^2 - 2V_k V_l \cos(\delta_k - \\ & \delta_l)) \end{aligned} \quad (20)$$

Where, nl is the total lines, $g_{k,l}$ is the transmission line conductance, V_l & V_k are the l^{th}&k^{th} buses' voltage magnitudes. The following is the expression for the total load bus voltage deviation:

$$f_3 = (VD) = \sum_{k=1}^{nl} (|V_k - 1|)^2 \quad (21)$$

The sum of the squared voltage stability index (L) at the load bus is written as:

$$f_4 = L_l = \left|1 — \sum_{k=1}^{ng} F_{lk} \frac{V_k}{V_l} \angle\theta_{kl} + \delta_k + \delta_l\right| \quad (22)$$

4.1. Equality Constraints

An OPF equality constraints are written as follows

4.1.1. Real Power Constraints

$$P_{GK} - P_{DK} - \sum_{l=1}^{n} |V_k||V_l||Y_{kl}| \cos(\theta_{kl} - \delta_k - \delta_l) = 0 \quad (23)$$

4.1.2. Reactive Power Constraints

$$Q_{GK} - Q_{DK} - \sum_{l=1}^{n} |V_k||V_l||Y_{kl}| \sin(\theta_{kl} - \delta_k - \delta_l) = 0 \quad (24)$$

Where $l \in [1, t]$ and t = total buses.

4.2. Inequality Constraints

The OPF inequality constraints include the limits set to maintain system security and the physical device constraints in the power system. The restrictions on inequality are as follows.

4.2.1. Generator Constraints

$$\left.\begin{aligned} P_{Gk}^{min} \le P_{Gk} \le P_{Gk}^{max} \\ V_{Gk}^{min} \le V_{Gk} \le V_{Gk}^{max} \\ Q_{Gk}^{min} \le Q_{Gk} \le Q_{Gk}^{max} \end{aligned}\right\} \quad (25)$$

Where $k \in [1, ng]$ and ng = number of generators

4.2.2. Transformer Constraints

The lower and upper limits of the tap setting of the Transformer are,

$$T_k^{min} \le T_k \le T_k^{max}, k = 1,2, \dots N_T \quad (26)$$

Where N_T is the total number of transformers

4.2.3. Constraints of Shunt Var Compensator

Limiting values of shunt var compensators are

$$Q_{ck}^{min} \le Q_{ck} \le Q_{ck}^{max}, k = 1,2, \dots ng \quad (27)$$

4.2.4. Security Constraints

$$V_{lk}^{min} \le V_{lk} \le V_{lk}^{max}, k = 1,2, \dots nl \quad (28)$$

$$S_{lk} \le S_{lk}^{max}, k = 1,2, \dots nl \quad (29)$$

4.2.5. C-UPFC FACTS Device Constraints

$$\left.\begin{aligned} V_r^{min} \le V_r \le V_r^{max} \\ V_{sh}^{min} \le V_{sh} \le V_{sh}^{max} \\ \delta_s^{min} \le \delta_s \le \delta_s^{max} \\ \delta_r^{min} \le \delta_r \le \delta_r^{max} \\ \delta_{sh}^{min} \le \delta_{sh} \le \delta_{sh}^{max} \end{aligned}\right\} \quad (30)$$

5. Proposed Method

This paper uses Opposition-based Modified Rao's algorithm to solve the optimal power flow problem, which is discussed in detail below.

5.1. Rao's Algorithm

Different new metaphor algorithms based on various natural occurrences or the behaviour of animals, musical instruments, cultures, fish, societies, insects, planets, etc., have recently inundated the population-based meta-heuristic algorithms field. Every month, many new optimization algorithms are proposed, with the authors claiming that their algorithms are 'better' than the competition. Some of these recently proposed algorithms are dying naturally since no one is using them, while others have had some degree of success.

However, this kind of research might be viewed as dangerous and may not help to develop the optimization profession. Instead of attempting to create algorithms based on metaphors, it would be preferable for researchers to concentrate on creating straightforward optimization techniques that can offer efficient answers to complex issues. In light of this, straightforward Rao's algorithms are shown with their algorithm-specific parameters.

Numerous unconstrained and constrained optimization issues are solved utilizing Rao's optimization strategies [26, 27]. [28] Rao algorithm applied for economic load dispatch problem. The worst and best solutions discovered during the optimisation process and the candidate solution interactions constitute the foundation of these algorithms. These algorithms don't need any algorithm-specific control parameters; they need standard control parameters like termination criteria and population size. The following describes how Rao's algorithm functions.

Let f(d) be the objective function's desired reduction (or maximized). Assume that there are m design variables and n possible solutions at every given iteration (i.e., population size, where k=1, 2..., n).

The greatest candidate should get the best value of f(d) (i.e., f(d)best) in all candidate solutions, and the worst candidate should get the worst value of f(d) (i.e., f(d)worst) in all candidate solutions. [26] The following equations modify the value of $d_{k.l.m}$, which is the value of the k^{th} variable for the l^{th} candidate during the m^{th} iteration.

$$d'_{k,l,m} = d_{k,l,m} + r_{1k,l}(d_{k,best,m} - d_{k,worst,m}) \quad (31)$$

5.1.1. Rao's Algorithm Steps

1. Read the input data like candidate size, total iterations, variable size, and minimum and maximum bounds of variables.
2. Randomly generate initial population or candidate solutions.
3. Assess each initial population's objective function.
4. From the initial solution, determine the worst and best options.

5. Update the population using equation (14).
6. Assess each updated population's objective function.
7. Compare the initial population with the updated population; if an updated population is better than the initial population, then replace the initial population with the updated population and update the worst and best solutions.
8. Otherwise, the initial population remains the same. Repeat the procedure from step 2 to step 8 until the criteria is satisfied.

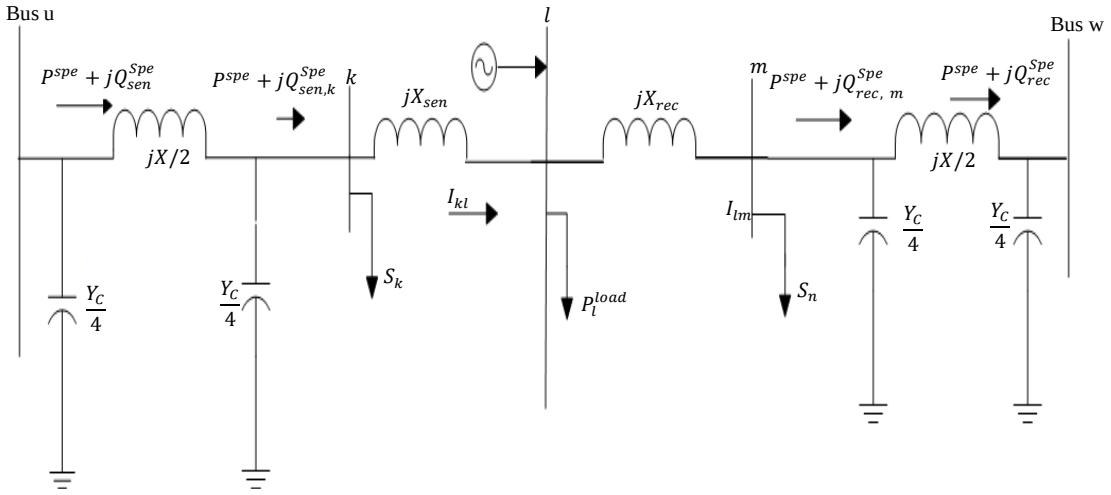

Fig. 4 C-UPFC power injected model

5.2. Opposition-Based Modified Rao's Algorithm

Opposition-Based Learning (OBL) [29] is a method that is frequently used to improve several optimization algorithms, including the Quasi-Opposite Bonobo Optimizer (QOBO) [30], the Quasi-Opposite Teaching-Learning Optimizer (QOTLBO) [31], and the oppositional jaya algorithm [32].

Figure 5 depicts the opposition-based modified Rao's method flowchart. By applying the candidate solution and the opposing one simultaneously, the OBL can be made better. As a result, in this study, the opposite solution of $d^{'i}_{i,j,k}$ in the Rao method will be expressed as

$$d^{'qi}_{i,j,k} = \begin{cases} C + r_1\left(C - d^{'}_{i,j,k}\right), |d^{'}_{i,j,k} < C \\ C + r_1\left(d^{'}_{i,j,k} — C\right), |d^{'}_{i,j,k} \geq C \end{cases} \quad (32)$$

Opposition-Based Generation Jumping: A new candidate solution may be selected by the evolutionary process, ideally more suitable than the existing one, by employing a comparable strategy on the current population.

After creating new folks through selection, The Most Mp fittest individuals are picked from the union of the existing population and the opposing population, which is decided based on a jumping rate gr (i.e., jumping probability).

Generation leaping determines the opposition population dynamically, in contrast to opposition-based initiation. Instead of using the variable's predefined interval limits, generation leaping determines each variable's opposition based on its lowest and highest values in the current population.

$$Od_{k,l} = min^p_l + max^p_l — d_{k,l} \quad (33)$$

Where $k = 1,2,\ldots,M_P, l = 1,2,\ldots,H$

Calculate the opposing population using the current interval of the variables ($[min^p_l, max^p_l)$] in the population, which, as the search continues, becomes significantly less than the corresponding starting range ($[a_j, b_j)$] , while remaining within the static interval boundaries of variables.

Randomized Local Search: Research has demonstrated that adding specific types of domain knowledge can significantly enhance the ability of evolutionary algorithms to search. Similar to how Rao's algorithm, built on the opposite, may be improved, non-evolutionary algorithms can also. A quick and effective direct search technique without the need for objective functions, analytical gradients, or numerical is the Randomized local search. The following definition applies to the proposed randomized local search.

$$d^*_{G,j,best} = d_{G,j,best} + 0.1\left(d^{max^{min}_{G-1,j}}_{G-1,j} Gauss(0,1), j \in [1,2,\ldots,H]\right) \quad (34)$$

Where $d_{G,best}$ is the top person in population G, $d_{G,j,best}$is the j[th] variable of $d_{G,best}$, $d^*_{G,j,best}$is the new trail

point, $d_{G-1,j}^{max}$ and $d_{G-1,j}^{min}$ in that order, the highest and lowest values of the j[th] variable in generation G-1. The random Gaussian variable Gauss (0, 1) has a unitary standard deviation and zero mean. The steps for randomized local search are as follows:

1. Find the worst and best individuals in the population, together with their function values: $d_{G,worst}$, $d_{G,best}$, f_w,f_b then set the local iteration number LocalK to 1.
2. Calculate $d_{G,best}^{*}$ as directed by the formula (35). Assess $f_b^* = f(d_{G,best}^{*})$ and decide Local k=Local K+1. While $(f_b^* > f_w \quad and \quad LocalK \leq ceil(\gamma.MP))$, Where γ is the multiplying factor and the operator termed as ceil (•) rounds input to the closest integers more prominent than or equal to the input.
3. Replace $d_{G,worst}$ by $d_{G,best}^{*}$ in the population, when $f_b^* < f_w$, when $f_b^* < f_w$.

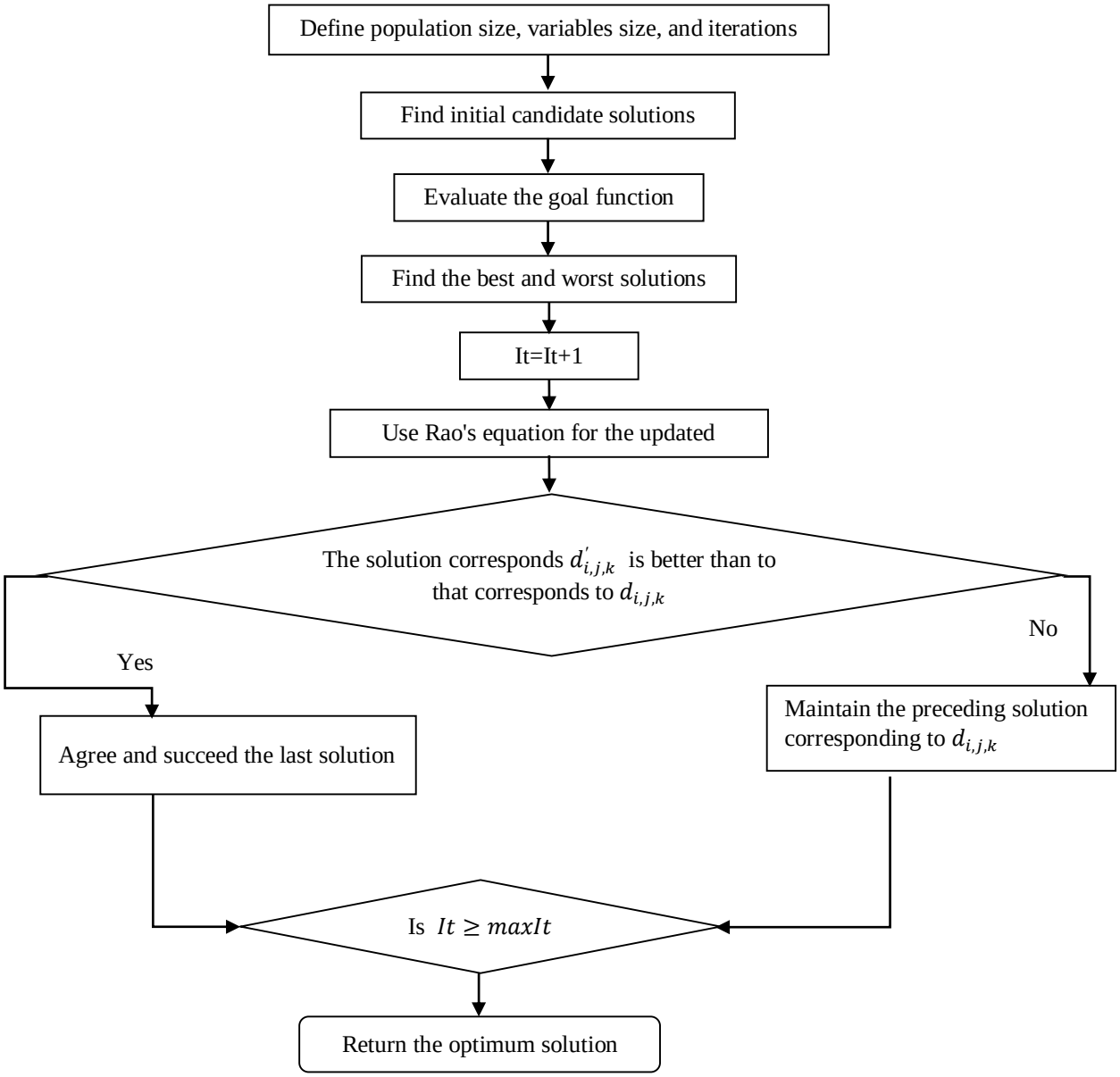

Fig. 5 Flow chart of Opposition-based Modified Rao's algorithm

The following is the pseudo-code for the modified RAO's algorithm based on the opposition:

1. Create a population with a uniform distribution d_0
2. for p = 0 to M_P do
3. for q= 0 to H do
4. $Od_{0p,q} \leftarrow d_q^{min} + d_q^{max} - d_{0p,q}$
5. Terminate for
6. Terminate for
7. Choose the M_P fittest persons and take the $\{d_0, od_0\}$as the beginning population.
8. while (it<$itmax$) do
9. Apply OMR development process: Contrary to the Current Population Arbitrary local search
10. if *rand (0, 1)* <gr (Jumping rate), then
11. for p = 0 to M_P do
12. for q = 0 to H do
13. $Od_{p,q} \leftarrow MIN_p^p + MAX_p^p - d_{p,q}$
14. Terminate for
15. Terminate for
16. Choose M_P fittest persons from the set $\{d, Od\}$as the beginning population d
17. Terminate if
18. Terminate while

6. OPF Solution Using OMR

The IEEE-30 bus test system includes four tap-setting transformers, six generators and 41 transmission lines. Data on the real and reactive power limits and the cost coefficients for each production unit is taken from [1], and the IEEE-30 bus system's overall load demand is 283.4 MW [1].

Figure 6 shows the load bus voltage profile graph with and without the C-UPFC device. The red line indicates the load bus voltage profile when the C-UPFC device is employed, and the Blue line indicates the load bus voltage profile when the C-UPFC device is not used. It is known from Figure 6 that the load bus voltage profile improved much better with the C-UPFC device than without it.

Figure 7 shows the load bus angle profile with and without the C-UPFC device. The red line indicates the load bus angle profile when the C-UPFC device is employed, and the Blue line indicates the load bus angle profile when the C-UPFC device is not used. It is known from Figure 7 that the load bus angle profile improved much better with the C-UPFC device than without it.

Figure 8 shows the real power graph with and without the C-UPFC device. The red line indicates the real power flow between the transmission lines when the C-UPFC device is employed, and the blue line indicates the real power flow between the transmission lines when the C-UPFC device is not used. It is known from Figure 8 real power flow between transmission lines improved much better with the C-UPFC device than without it.

Figure 9 shows the reactive power graph with and without the C-UPFC device. The red line indicates the Reactive power flow between the transmission lines when the C-UPFC device is employed, and the blue line indicates the reacti0076e power flow between the transmission lines when the C-UPFC device is not used. It is known from Figure 9 that reactive power flow between transmission lines improved much better with the C-UPFC device than without it.

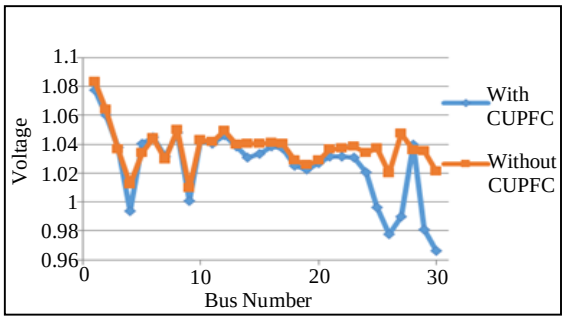

Fig. 6 Comparison graph of load bus voltage profile without and with C-UPFC at lines 25-26 using OMR algorithm

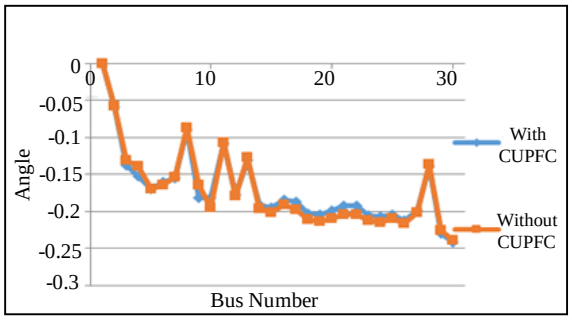

Fig. 7 Comparison graph of load bus angle profile without and with C-UPFC at lines 25-26 using OMR algorithm

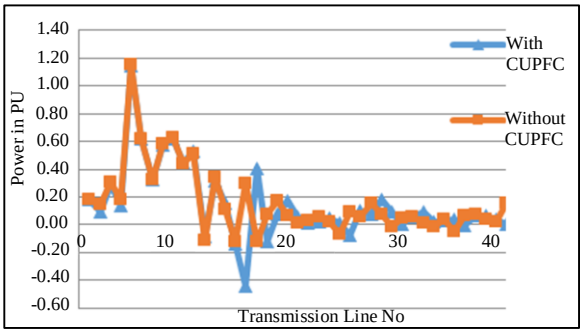

Fig. 8 Comparison graph of real power flow without and with C-UPFC at lines 25-26 using OMR algorithm

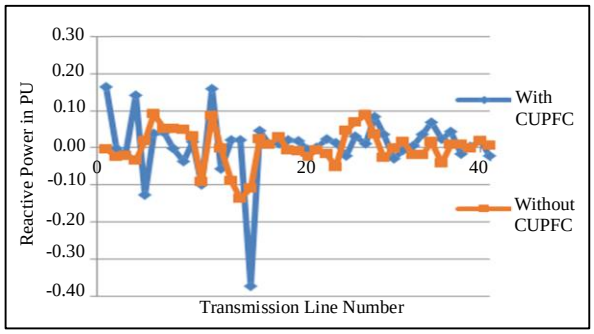

Fig. 9 Comparison of reactive power flow without and with C-UPFC at lines 25-26 using OMR algorithm

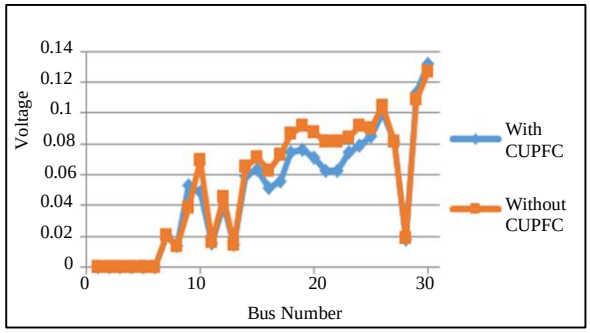

Fig. 10 Comparison of voltage stability index without and with C-UPFC at line 25-26 voltage stability index using OMR algorithm

Figures 11-14 show the convergence characteristics of each objective function, i.e. the total fuel cost of generation, active power losses, the sum of the squared voltage stability index, and the entire bus voltage deviation for the IEEE-30 bus system without and with the C-UPFC device at line 25-26 and the objective functions converged smoothly to the optimum value without any abrupt oscillations. This shows the convergence reliability of the proposed OMR algorithm without and with the C-UPFC device.

Figure 11 shows the convergence characteristics of the fuel cost of generation of the IEEE-30 bus system under normal operating conditions. The minimum price obtained with the OMR algorithm is 788.0304 $/hr.

Figure 12 shows the convergence characteristics of total real power loss for the IEEE-30 bus system under normal operating conditions. The minimum power loss obtained by the OMR algorithm is 0.02426 p.u.

Figure 13 shows the convergence characteristics of the sum of the squared voltage stability index for the IEEE-30 bus system under normal operating conditions. The minimum voltage stability index objective function obtained by the OMR algorithm is 0.1007. Figure 14 shows the voltage deviation convergence characteristics of the IEEE-30 bus system under normal operating conditions. The minimum voltage deviation obtained by the OMR algorithm is 0.0459 p.u.

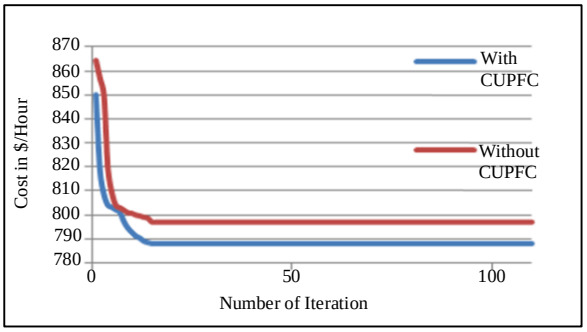

Fig. 11 Convergence characteristics of total generation cost without and with C-UPFC at line 25-26 using OMR algorithm

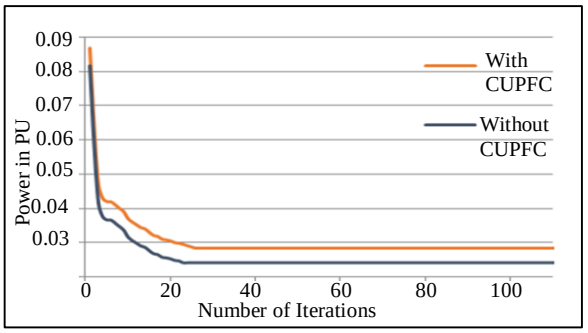

Fig. 12 Convergence characteristics of real power loss without and with C-UPFC at line 25-26 using OMR algorithm

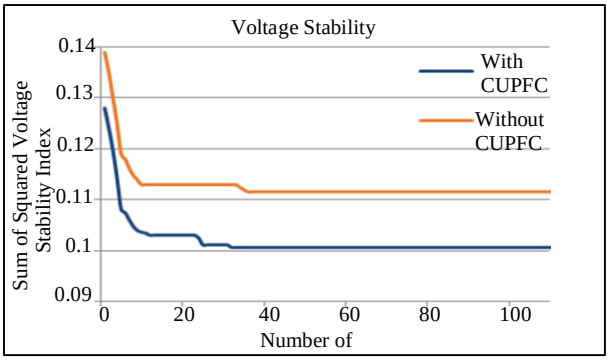

Fig. 13 Convergence characteristics of voltage stability index without and with C-UPFC at line 25-26 using OMR algorithm

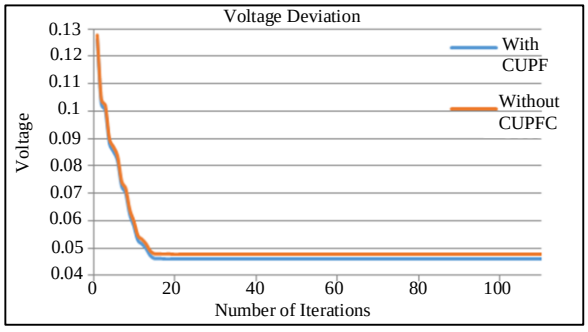

Fig. 14 Convergence characteristics of voltage deviation without and with C-UPFC at line 25-26 using OMR algorithm

Table 1 shows the performance parameters of the system using the proposed OMR algorithm with and without a C-UPFC device at lines 25-26. The results clearly show

that the proposed OMR algorithm gives more optimum values. The results of the proposed OMR algorithm are compared with AGOA, GOA, MRao-2, and MJAYA algorithms in Table 2 when the C-UPFC device is not included. The fuel cost values obtained by the AGOA, GOA, MRao-2, and MJAYA algorithms are 800.0212 $/h, 800.9728 $/h, 800.4412 $/h, and 833.3410 $/h, respectively. It is reduced to 797.0928 $/h by the OMR algorithm, and total voltage deviation and power losses are significantly reduced by the OMR algorithm than the above mentioned techniques.

Table 3 compares the suggested approach OMR with the AGOA and GOA optimization techniques when the C-UPFC device is included. Due to the addition of the C-UPFC device, the fuel cost value using the OMR algorithm is reduced from 799.0928 $/h to 788.0304 $/h and total voltage deviation and power losses are also reduced well.

Table 1. Performance parameters comparison for IEEE 30-bus test system without and with C-UPFC at lines 25-26

Optimization Method	Performance Parameters	Cost		Power Loss		Voltage Deviation		Voltage Stability Index	
		Without	With	Without	With	Without	With	Without	With
Proposed OMR	Fuel Cost ($/hr.)	797.0928	788.0304	966.09	964.3	802.74	802.94	799.49	796.85
	Real Power Loss (pu)	0.083	0.0817	0.02839	0.02426	0.09612	0.0909	0.0842	0.0506
	∑ Voltage Deviation (pu)	1.7238	1.648	0.7809	0.747	0.0479	0.0459	1.9641	1.829
	L-Index	0.1156	0.1145	0.1145	0.1117	0.1139	0.0959	0.1116	0.1007

Table 2. Comparison of OMR algorithm with MRao-2, AGOA, GOA, and MJAYA algorithms without C-UPFC

Variables	GOA	AGOA	MRao-2	MJAYA	OMR
Pg1	1.75494	1.75768	1.7636	1.7636	1.7458
Pg2	0.48457	0.48678	0.4907	0.4907	0.5742
Pg3	0.21391	0.21292	0.2124	0.2124	0.1938
Pg4	0.21935	0.20698	0.2137	0.2137	0.1000
Pg5	0.13139	0.13736	0.1221	0.1221	0.2000
Pg6	0.12	0.12	0.1210	0.1210	0.1200
Vg1	1.0707	1.0868	1.083304	1.083304	1.1000
Vg2	1.0547	1.0655	1.092657	1.092657	1.0877
Vg3	1.0263	1.0331	1.029766	1.029766	1.0688
Vg4	1.0338	1.0398	1.037062	1.037062	1.0796
Vg5	1.0442	1.0764	1.059477	1.059477	1.0614
Vg6	1.0084	1.0377	1.046984	1.046984	1.1000
T1	1.0963	0.99187	1.002334	1.002334	0.9685
T2	1.0825	0.98616	0.953247	0.953247	1.1000

T3	1.0986	0.95596	0.971027	0.971027	0.9624
T4	1.0233	0.98354	0.971058	0.971058	0.9593
Qc1	0.027123	0.043112	3.7024	3.7024	0.0908
Qc2	0.011816	0.040136	2.0306	2.0306	0
Qc3	0.031861	0.045024	2.2152	2.2152	0.0751
Qc4	0.03485	0.0015095	4.6995	4.6995	0.0786
Qc5	0.05	0.0066628	3.859	3.859	0.0422
Qc6	0.0016044	0.034307	4.8858	4.8858	0.0141
Qc7	0.021017	0.013081	3.9984	3.9984	0
Qc8	0.039768	0.041318	4.8289	4.8289	0.0340
Qc9	0.032786	0.032445	1.6698	1.6698	0.0240
Cost ($/h)	800.9728	800.0212	800.4412	833.3410	797.0928
VD (p.u)	0.8874	0.7695	0.868108	0.1196	0.0479
Ploss (MW)	0.090149	0.087726	0.08993	0.051779	0.02839

Table 3. Comparison of OMR algorithm with AGOA, and GOA algorithms with C-UPFC

Variables	AGOA	GOA	OMR
Pg1	1.79945	1.78617	1.8061
Pg2	0.47696	0.47094	0.2311
Pg3	0.21363	0.20822	0.1343
Pg4	0.17655	0.1453	0.2403
Pg5	0.11324	0.1733	0.2791
Pg6	0.12001	0.12	0.1431
Vg1	1.0535	1.039	1.0617
Vg2	1.041	1.0275	1.0405
Vg3	1.0121	0.99626	1.0289
Vg4	1.0225	1.014	1.0314
Vg5	1.0866	1.0228	1.0579
Vg6	1.0532	1.0692	1.0216
T1	1.0434	1.044	0.9467
T2	0.90216	0.97652	0.9694
T3	0.97855	1.0063	0.9521
T4	0.95103	0.93612	0.9013
Qc1	0.019543	0.020582	0.064
Qc2	0.041751	0.025143	0
Qc3	0.0011015	0.029311	0.053
Qc4	0.019298	0.032317	0.0464
Qc5	0	0.027383	0.0214
Qc6	0.0203	0.049929	0.0259
Qc7	0	0	0
Qc8	0.008125	0.0020032	0.0083
Qc9	0.16702	0.029547	0.01465
Cost ($/h)	791.222	794.0913	788.0304
VD (p.u.)	0.5949	0.2738	0.0459
Ploss (p.u.)	0.06582	0.069919	0.02426

7. Conclusion

This paper solves the OPF problem without and with C-UPFC using an Opposition-based Modified Rao's (OMR) algorithm with lower and upper thermal unit restrictions, transformer tap settings, q-shunts, and bus voltage limits. The IEEE-30 bus test system was used to evaluate OMR's

efficacy. The obtained results by applying the OMR algorithm are compared with techniques like AGOA, MRAO-2 and PSO algorithms. The results obtained by the proposed OMR algorithm are better than the algorithms. Therefore, the OMR algorithm has better results, faster convergence characteristics and requires less computational time than the other techniques. The minimum fuel cost obtained by the OMR algorithm without C-UPFC is 797.0928. It is better than the fuel cost received by [21], and when C-UPFC included fuel cost obtained with the OMR algorithm is reduced from 797.00928 $/h (without C-UPFC) to 788.0304 $/h (with C-UPFC) and also power losses are reduced, and improved the voltage profile and real and reactive power flows.

References

[1] Tankut Yalcinoz, and Krzysztof Rudion, "Multi-Objective Environmental-Economic Load Dispatch Considering Generator Constraints and Wind Power Using Improved Multi-Objective Particle Swarm Optimization," *Advances in Electrical and Computer Engineering*, vol. 20, no. 4, pp. 3-10, 2020. [CrossRef] [Google Scholar] [Publisher Link]

[2] Hong Gong, Xiongfei Wang, and Dongsheng Yang, "Small Signal Model of STATCOM and Its Model Validation," *IEEE Power and Energy Society General Meeting (PESGM)*, Portland, OR, USA, pp. 1-5, 2018. [CrossRef] [Google Scholar] [Publisher Link]

[3] Valeriya Tuzikova, Josef Tlusty, and Zdenek Muller, "A Novel Power Loses Reduction Method Based on a Particle Swarm Optimization Algorithm Using STATCOM," *Energies*, vol. 11, no. 10, pp. 1-15, 2018. [CrossRef] [Google Scholar] [Publisher Link]

[4] Nikolay Djagarov et al., "Mathematical Model for the Study of Low-Voltage Ride through of Wind Permanent Magnet Synchronous Generator by Means of STATCOM," *20th International Scientific Conference on Electric Power Engineering (EPE)*, Kouty nad Desnou, Czech Republic, pp. 1-5, 2019. [CrossRef] [Google Scholar] [Publisher Link]

[5] Susanta Dutta, Provas Kumar Roy, and Debashis Nandi, "Optimal Allocation of Static Synchronous Series Compensator Controllers Using Chemical Reaction Optimization for Reactive Power Dispatch," *International Journal of Energy Optimization and Engineering*, vol. 5, no. 3, pp. 1-20, 2016. [CrossRef] [Google Scholar] [Publisher Link]

[6] Jalpesh H. Limbola, and Mehul D. Solanki, "Modelling and Control of SSSC to Enhance the Power Transmission Capacity," *2018 2nd International Conference on Trends in Electronics and Informatics (ICOEI)*, Tirunelveli, India, pp. 647-651, 2018. [CrossRef] [Google Scholar] [Publisher Link]

[7] Mustafa Şeker, Arif Memmedov, and Rafael Hüseyinov, "The Modelling and Simulation of Static VAR Compensator (SVC) System Electric Arc Furnace with Matlab/Simulink," *2016 National Conference on Electrical, Electronics and Biomedical Engineering (ELECO)*, Bursa, Turkey, pp. 262-268, 2016. [CrossRef] [Google Scholar] [Publisher Link]

[8] Rakesh Kushwah, and Mandakini Gupta, "Modelling and Simulation of SVC and STATCOM for Enhancement of Power System Transient Stability Using Matlab," *2016 International Conference on Electrical, Electronics, and Optimization Techniques (ICEEOT)*, Chennai, India, pp. 4041-4045, 2016. [CrossRef] [Google Scholar] [Publisher Link]

[9] N. Kalpana, and Venu Gopala Rao M., "A Standardized Approach for Evaluating UPFC'S Optimal Location Using Metaheuristic Algorithms to Improve Power Quality," *2022 International Conference on Electronics and Renewable Systems (ICEARS)*, Tuticorin, India, pp. 104-110, 2022. [CrossRef] [Google Scholar] [Publisher Link]

[10] M. Balasubbareddy, and Divyanshi Dwivedi, "Incorporation of Current Injection Modelling of UPFC and Analyzing Power Flow Solution Using Criss Cross Optimization Algorithm," *2019 IEEE International Conference on Electrical, Computer and Communication Technologies (ICECCT)*, Coimbatore, India, pp. 1-6, 2019. [CrossRef] [Google Scholar] [Publisher Link]

[11] P. Balachennaih, and P. Nagendra, "Firefly Algorithm Based Multi-Objective Using OUPFC in a Power System," *TENCON 2017 - 2017 IEEE Region 10 Conference*, Penang, Malaysia, pp. 2901-2906, 2017. [CrossRef] [Google Scholar] [Publisher Link]

[12] Zulkiffli Abdul Hamid et al., "Mitigation of Voltage Level and Real Power Loss in Transmission System via Optimal UPFC Placement," *2022 IEEE International Conference in Power Engineering Application (ICPEA)*, Shah Alam, Malaysia, pp. 1-6, 2022. [CrossRef] [Google Scholar] [Publisher Link]

[13] Ehad E. Elatter, and Salah K. ElSayed, "Modified JAYA Algorithm for Optimal Power Flow Incorporating Renewable Energy Sources Considering the Cost, Emission, Power Loss and Voltage Profile Improvement," *Energy*, vol. 178, pp. 598-609, 2019. [CrossRef] [Google Scholar] [Publisher Link]

[14] Harish Pulluri, R. Naresh, and Veena Sharma, "An Enhanced Self-Adaptive Differential Evolution-Based Solution Methodology for Multi-Objective Optimal Power Flow," *Applied Soft Computing*, vol. 54, pp. 229-245, 2017. [CrossRef] [Google Scholar] [Publisher Link]

[15] Mohamed H. Hasan et al., "A Modified Rao-2 Algorithm for Optimal Power Flow Incorporating Renewable Energy Sources," *Mathematics*, vol. 9, no. 13, pp. 1-22, 2021. [CrossRef] [Google Scholar] [Publisher Link]

[16] Sharyar Rahnamayan, Hamid R. Tizhoosh, and Magdy M.A. Salama, "Opposition-Based Differential Evolution Algorithm," *IEEE Transaction on Evolutionary Computation*, vol. 12, no. 1, pp. 64-79, 2008. [CrossRef] [Google Scholar] [Publisher Link]

[17] Dany Varghese, and Varaprasad Janamala, "Optimal Location and Parameters of GUPFC for Transmission Loss Minimization Using PSO Algorithm," *2017 Innovations in Power and Advanced Computing Technologies (i-PACT)*, Vellore, India, pp. 1-6, 2017. [CrossRef] [Google Scholar] [Publisher Link]

[18] Ayman Awad et al., "GUPFC Modeling for Flow Analysis in MVDC Grids," *2021 IEEE International Conference on Environmental and Electrical Engineering and 2021 IEEE Industrial and Commercial Power Systems Europe (EEEIC/I&CPS EUROPE)*, Bari, Italy, pp. 1-5, 2021. [CrossRef] [Google Scholar] [Publisher Link]

[19] B.T. Ooi et al., "Mid-Point Sitting of FACTS Devices in Transmission Lines," *IEEE Transactions on Power Delivery*, vol. 12, no. 4, pp. 1717-1722, 1997. [CrossRef] [Google Scholar] [Publisher Link]

[20] Boon Teck Ooi, and Bin Lu, "C-UPFC: A New FACTS Controller with 4 Degrees of Freedom," *2000 IEEE 31st Annual Power Electronics Specialists Conference. Conference Proceedings (Cat. No.00CH37018)*, Galway, Ireland, vol. 2, pp. 961-966, 2000. [CrossRef] [Google Scholar] [Publisher Link]

[21] A. Ajami et al., "Modelling and Control of C-UPFC for Power System Transient Studies," S*imulation Modelling Practice and Theory*, vol. 14, no. 5, pp. 564-576, 2006. [CrossRef] [Google Scholar] [Publisher Link]

[22] S. Kamel, F. Jurado, and R. Mihalic, "Advanced Modelling of Centre-Node Unified Power Flow Controller in NR Load Flow Algorithm," *Electric Power Systems Research*, vol. 121, pp. 176-182, 2015. [CrossRef] [Publisher Link]

[23] Salah Kamel et al., "A Comprehensive Model of C-UPFC with Innovative Constraint Enforcement Techniques in Load Flow Analysis," *International Journal of Electrical Power & Energy Systems*, vol. 101, pp. 289-300, 2018. [CrossRef] [Google Scholar] [Publisher Link]

[24] Ayman Alhejji et al., "Optimal Power Flow Solution with an Embedded Center-Node Unified Power Flow Controller Using an Adaptive Grasshopper Optimization Algorithm," *IEEE Access*, vol. 8, pp. 119020-119037, 2020. [CrossRef] [Google Scholar] [Publisher Link]

[25] Ashraf Mostafa et al., "Optimal Power Flow Solution Using Levy Spiral Flight Equilibrium Optimizer with Incorporating CUPFC," *IEEE Access*, vol. 9, pp. 69985-69998, 2021. [CrossRef] [Google Scholar] [Publisher Link]

[26] Niharika Agrawal, and Mamatha Gowda, "Power Flow Enhancement by TCSC Using Two Different Types of Pulse Generators," *International Journal of Recent Engineering Science*, vol. 9, no. 1, pp. 31-38, 2022. [CrossRef] [Google Scholar] [Publisher Link]

[27] Ravipudi Venkata Rao, "Rao Algorithms: Metaphor-less Simple Algorithms for Solving Optimization Problems," *International Journal of Industrial Engineering Computations*, vol. 11, no. 1, pp. 107-130, 2020. [CrossRef] [Google Scholar] [Publisher Link]

[28] Wenqei Wei et al., "A Behaviour-Selection Based Rao Algorithm and Its Applications to Power System Economic Load Dispatch Problems," *Applied Intelligence*, vol. 52, pp. 11966-11999, 2022. [CrossRef] [Google Scholar] [Publisher Link]

[29] H.R. Tizhoosh, "'Opposition-Based Learning: A New Scheme for Machine Intelligence," *International Conference on Computational Intelligence for Modelling, Control and Automation and International Conference on Intelligent Agents, Web Technologies and Internet Commerce (CIMCA-IAWTIC'06)*, Vienna, Austria, pp. 695-701, 2005. [CrossRef] [Google Scholar] [Publisher Link]

[30] Sharmistha Sharma, Subhadeep Bhattacharjee, and Aniruddha Bhattacharya, "Quasi-Oppositional Swine Influenza Model Based Optimization with Quarantine for Optimal Allocation of DG in Radial Distribution Network," *International Journal of Electrical Power & Energy Systems*, vol. 74, pp. 348-373, 2016. [CrossRef] [Google Scholar] [Publisher Link]

[31] Sneha Sultana, and Provas Kumar Roy, "Multi-Objective Quasi-Oppositional Teaching Learning Based Optimization for Optimal Location of Distributed Systems," *International Journal of Electrical Power & Energy Systems*, vol. 63, pp. 534-545, 2014. [CrossRef] [Google Scholar] [Publisher Link]

[32] Jiangtao Yu, Chang-Hwan Kim, and Sang-Bong Rhee, "Oppositional Jaya Algorithm with Distance-Adaptive Coefficient in Solving Directional over Current Relays Coordination problem," *IEEE Access*, vol. 7, pp. 150729-150742, 2019. [CrossRef] [Google Scholar] [Publisher Link]